Inorganic Chemistry

Article

pubs.acs.org/IC

P(CH)P Pincer Rhodium(I) Complexes: The Key Role of Electron-Poor Imidazoliophosphine Extremities

Cécile Barthes,[†,‡] Christine Lepetit,[†,‡] Yves Canac,*[,†,‡] Carine Duhayon,[†,‡] Davit Zargarian,[§] and Remi Chauvin*[,†,‡]

[†]CNRS, LCC (Laboratoire de Chimie de Coordination), 205, route de Narbonne, F-31077 Toulouse, France

[‡]Université de Toulouse, UPS, INP, LCC, F-31077 Toulouse, France

[§]Département de Chimie, Université de Montréal, Montréal, Québec H3C 3J7, Canada

Supporting Information

ABSTRACT: The coordination chemistry of a potentially pincer-type dicationic *meta*-phenylene-bis(imidazoliophosphine) ligand **3** to neutral and cationic carbonylrhodium(I) centers has been investigated. Similarly to what was observed previously for its *ortho*-phenylene counterpart, **3** was found to bind to the RhCl(CO) fragment in a trans-chelating manner that makes possible a weak Rh−C(H) interaction, inferred from the non-bonding but relatively short Rh−C and Rh−H contacts observed in the solid state structure of the dicationic adduct (**3**)RhCl(CO) (**5**). Formation of the target PCP-type pincer complex could not be triggered despite multiple attempts to deprotonate the central C−H moiety in the initial dicationic adduct **5**, or in the tricationic species $[(\mathbf{3})Rh(CO)]^{+}$ (**8**) generated by abstraction of the chloride ion from **5**. Complex **8** was identified on the basis of NMR and IR analyses as a Rh(I)-stabilized P(CH)P-intermediate en route to the anticipated classical PCP-type pincer complex. Analysis of the electronic structure of this intermediate computed at the density functional level of theory (DFT level) revealed a bonding overlap between a Rh d-orbital and π-orbitals of the *m*-phenylene ring. NBO analyses and calculated Wiberg indices confirm that this interaction comprises an η^1-C−Rh bonding mode, with only secondary contributions from the geminal C and H atoms. Although the target PCP-type pincer complex could not be generated, treatment of the tricationic intermediate with methanol induced a P−CN_2 bond cleavage at both imidazoliophosphine moieties, resulting in the formation of a dicationic "open pincer" species, that is, a nonchelated bis((MeO)PPh_2)-stabilized aryl-Rhodium complex that is the κC-only analogue of the putative κP,κC,κP-PCP complex sought initially. Theoretical studies at the DFT level of experimental or putative species relevant to the final C−H activation process ruled out the oxidative addition pathway. Two alternative pathways are proposed to explain the formation of the "open pincer" complex, one based on an organometallic α-elimination step, the other based on an organic aromatization-driven β-elimination process.

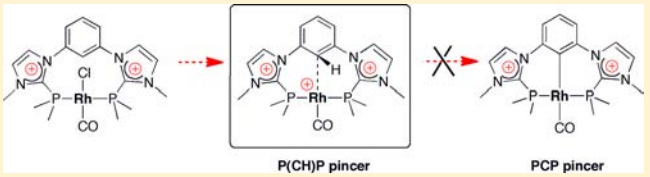

1. INTRODUCTION

Rigid tripodal ligands and their transition metal complexes are deserving of the generic appellation "pincer" owing to their unique robustness, enhanced catalytic properties, and diversity.[1] Strictly speaking, the term "pincer" currently refers to a tridentate ligand of the LXL′ type (in the Green formalism), that binds to metals in a double chelating *mer* fashion, which offers added protection against hydrolytic or oxidative cleavage. Their attractive reactivity and material properties apart, the synthesis of pincer complexes is of topical interest, in particular the key-process of X-metal bond formation when the X center is the central carbon atom of a *meta*-L,L′-disubstituted phenyl core. The kinetic and thermodynamic stability of such LCL′-type pincer complexes is determined not only by the tripodal chelating mode and the sp^2 hybridization state of the anionic C atom, but also by the nature of L and L′, which may be P-, N-, S-, Se-, or C-centered donor fragments with various steric and electronic demands. Among the latter, electron-donating trialkyl- phosphinyl arms are the most popular constituents of "electron-rich PCP pincers" **A** (Scheme 1).[2] More recently, the complementary category of "electron-poor PCP pincers" **B** has been exemplified by the introduction of strongly π-accepting phosphanyl arms, like fluoroalkyl-[3] and aryl-phosphanes,[4] N-pyrrolylphosphanes,[5] phosphites,[6] and, to a lesser extent, phosphoramidites[7] and phosphinites.[8]

Scheme 1. Typology of Transition Metal Pincer Complexes, Featuring Either an Electron-Rich Tridentate P-Csp^2-P Ligand A (*left*), or an Electron-Poor Tridentate P-Csp^2-P Ligand B (*right*)

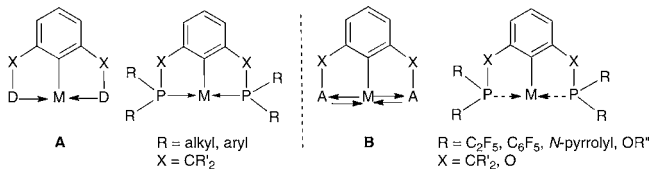

In the design of optimal ligands for catalysis, a single type of coordinating moiety with extreme donating character (strong or weak)

Received: March 28, 2012
Published: December 24, 2012

Scheme 2. Selective Sequential Phosphinylation and Methylation of 1,3-Bis(imidazolyl)benzene 1

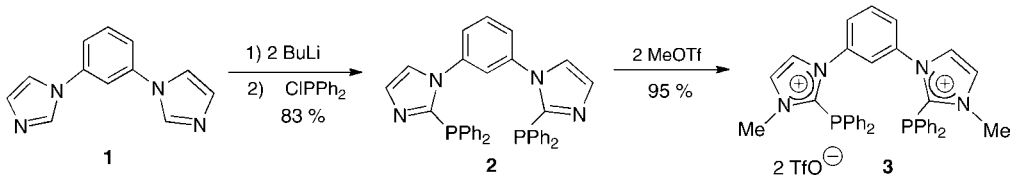

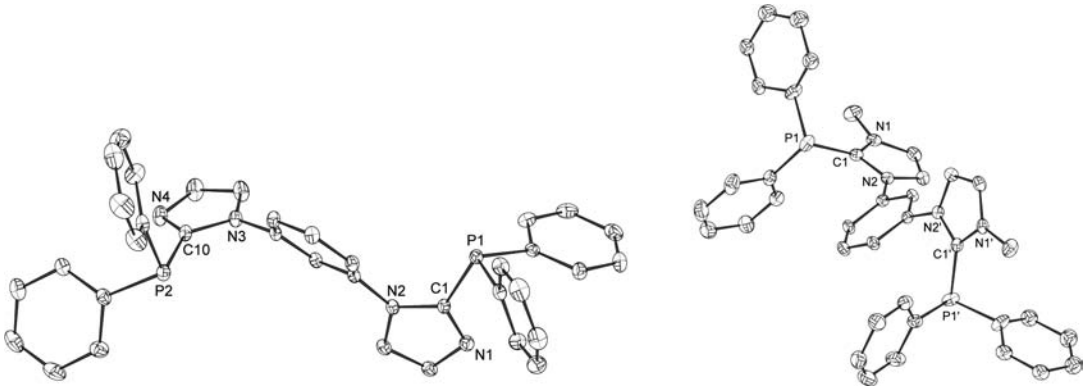

Figure 1. Molecular views of the X-ray crystal structures of the neutral and dicationic diphosphines **2** (*left*) and **3** (*right*), with thermal ellipsoids drawn at the 30% probability level (for clarity, the triflate anions and the H atoms are omitted). Selected bond distances (Å) and angles (deg). **2**: C1−P1 1.8266(18), C10−P2 1.8222(19), N1−C1 1.319(2), N2−C1 1.382(2), N1−C1−N2 110.39(15), N2−C1−P1 124.51(13). **3**: C1−P1 1.833(4), N1−C1 1.360(5), N2−C1 1.368(4), N1−C1−N2 104.5(3), N2−C1−P1 121.5(3).

might be too limiting because transition metal centers must satisfy varying criteria for achieving selectivity and activity over all the steps in a given catalytic cycle.[9] Along this direction, PCP pincers of type **B** might exhibit not only particular catalytic properties, but also peculiar photophysical properties resulting from a possible C→M→L_2 charge transfer of the "LMLCT" type. Perfluoroalkyl-P-substituted PCP pincers stand as the most π-accepting examples reported hitherto,[3] but since, in a very broad sense, cationic centers are more electronegative than fluorine atoms (basically because the range of the second ionization potentials is strictly higher than the range of the first ionization potentials), the introduction of imidazolium P-substituents could generate an attractive new familly of stable pincers of the P^+CP^+ variety. Imidazoliophosphanes are indeed more accurately described as NHC→phosphenium adducts,[10] where the positive charge formally located on the Lewis acceptor P center (instead of the α-position as in generic carbeniophosphanes[11]) illustrates the decrease of the electron resource and thus of the donor ability of the P ligand. Moreover, because of the rigid frame of the pincer structure, the expected trans- arrangement of the two P^+ moieties should be compatible with the formal electrostatic repulsion between the positive charges.

In this context, a systematic investigation of the coordination chemistry of P^+,P^+-chelating bis(imidazoliophosphine) ligands has been initiated. A recent report has documented how such a ligand based on the *o*-phenylene bridge can behave as a versatile cis- or trans-chelating ligand for Rh(I) centers depending on the electronic endowment of the latter: trans-chelating at a soft neutral RhCl(CO) center, cis-chelating at a harder cationic $[Rh(MeCN)_2]^+$ center.[12] As a follow-up to these ongoing studies and with the ultimate goal of developing the afore-proposed category of elusive P^+CP^+ pincer ligands, the coordination chemistry of a P^+,P^+-chelating bis(imidazoliophosphine) ligand based on the *m*-phenylene bridge has been examined. The present contribution addresses the coordinating behavior of this a priori less rigid ligand toward Rh(I) centers using both experimental and theoretical investigation tools.

2. RESULTS AND DISCUSSION

2.1. Experimental Results. Double deprotonation of the readily available 1,3-bis(imidazolyl)benzene **1**[13] with 2 equiv of *n*-BuLi in tetrahydrofuran (THF), followed by addition of a stoichiometric amount of chlorodiphenylphosphine afforded the neutral diphosphine **2** in 83% yield. Upon subsequent treatment with 2 equiv of methyl triflate (MeOTf) in CH_2Cl_2, the targeted dicationic diphosphine **3** was readily obtained in 95% yield (Scheme 2). The ionic structure of **3** was reflected in its low solubility in nonpolar solvents. The symmetric structures of **2** and **3** were indicated by the singlet resonances in their ^{31}P NMR spectra (δ_p = −30.2 ppm and δ_p = −21.0 ppm, respectively). A singlet resonance appearing at +3.52 ppm in the ^1H NMR spectrum of **3** was assigned to the N−CH_3 protons. The solid state structures of **2** and **3** were determined by X-ray diffraction analysis of colorless single crystals obtained from recrystallization in CH_2Cl_2/toluene (**2**) or CH_3CN/Et_2O (**3**). Molecular views and selected structural parameters are shown in Figure 1.[14]

The bis(imidazoliophosphine) **3** was then reacted with 0.5 equiv of $[RhCl(cod)]_2$ in CH_2Cl_2 (cod = 1,5-cyclooctadiene). The ^{31}P NMR spectrum of the reaction mixture showed the complete disappearance of **3**, and the appearance in a 1:4 ratio of two resonances at lower field (d, δ_p = +27.4 ppm, J_{PRh} = 149.9 Hz; d, δ_p = +26.3 ppm, J_{PRh} = 151.9 Hz): these signals were tentatively attributed to the formation of the expected 18-electron Rh(I) complex **4** (Scheme 3) that may adopt two geometrical configurations allowed by the chelating mode of the cod ligand: equatorial−equatorial or axial−equatorial. In each isomer, the observed equivalence of the two phosphorus atoms implies that they occupy two axial or two equatorial equivalent positions, while the cod ligand would thus be chelating in either equatorial−equatorial or axial−equatorial mode, respectively. The reluctance of the dicationic diphosphine **3** for the axial−equatorial chelating

dx.doi.org/10.1021/ic3006508 | *Inorg. Chem.* 2013, 52, 48−58

Scheme 3. Preparation of Dicationic Rhodium Complexes 4−5 of the Bis(amidiniophosphine) Ligand 3

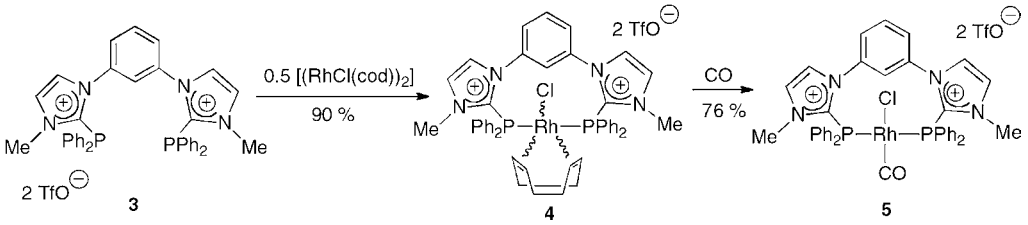

mode could indeed be dictated by the formal +/+ electrostatic repulsion, as recently invoked to explain the trans-chelating preference of the *o*-phenylene-bridged isomer of **3** in the palladium series.[12b] Complex **4** was isolated and characterized by spectroscopy, HRMS, and by derivatization to a CO adduct. Thus, bubbling CO through a CH_2Cl_2 solution of the isomeric mixture of **4** followed by NMR analysis indicated the conversion of the precursor ^{31}P resonances to a unique signal at +18.7 ppm (d, J_{PRh} = 135.7 Hz). In addition, a unique ^{13}C NMR signal was observed at δ_C = +182.9 ppm (td, J_{RhC} = 74.2 Hz, J_{PC} = 15.1 Hz), indicating a single type of CO ligand. These observations are in agreement with the expected symmetrical structure of complex **5** (Scheme 3). This new derivative was isolated in 76% yield and fully characterized, including by X-ray diffraction analysis performed on yellow crystals deposited from a MeCN/Et_2O mixture (Figure 2).[14]

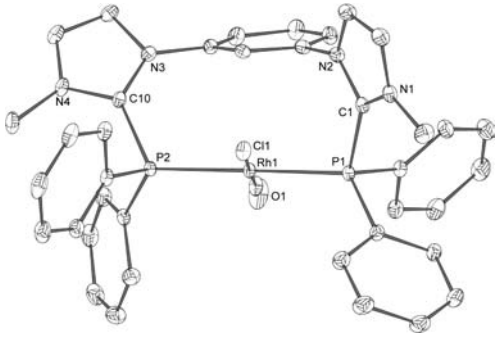

Figure 2. Molecular view of the X-ray crystal structure of the Rh(I) complex **5**, with thermal ellipsoids drawn at the 30% probability level (for clarity, the triflate anions and the H atoms are omitted). Selected bond distances (Å) and angles (deg). **5**: C1−P1 1.8472(17), C10−P2 1.8402(16), N1−C1 1.3420(19), N2−C1 1.358(2), P1−Rh1, 2.3107(4) P2−Rh1, 2.2998(4), Cl1−Rh1, 2.3700(4), C1−P1−Rh1 102.80(5), N1−C1−N2 106.30(14), P1−Rh1−P2 176.80(16), Cl1−Rh1−O1 178.83(5).

The Rh(I) atom in the solid state structure of **5** was found at the center of a quasi-square-planar environment, where the trans-arrangement of the two imidazoliophosphine moieties is confirmed by the P−Rh−P and CO−Rh−Cl angles of 176.80° and 178.83°, respectively. It is also worth noting here that while the Rh···C1 and Rh···H1 distances of about 2.77 Å are definitely nonbonding, they are shorter than the corresponding sums of van der Waals radii (see Section 2.2, Figure 3 and Table 1).

A rationale for the presence of a single CO ligand in trans position to the chloride ligand is a competition between the strong π-accepting character of the former and the electron-poor character of the "perpendicular" trans-chelating ligand **3**, both disfavoring spontaneous displacement of the Cl^- ligand from a Rh^+ center. The single ν_{CO} IR stretching frequency of RhCl(CO) complexes is commonly used for estimating the donor character of coligands,[15] and the measured value for **5** at 2005 cm^{-1} is of the same order of magnitude as those reported for *trans*-RhCl(CO)$[P(OMe)_3]_2$ (2011 cm^{-1}),[16] and for the closely related *trans*-bis(imidazoliophosphine) complexes **6** (2003 cm^{-1}),[17] and **7** (2007 cm^{-1}).[12a] These results indicate that the σ-donor vs π-acceptor character of imidazoliophosphine ligands is similar to that of phosphite ligands, whatever the bridge constraint (Scheme 4). Since, the *o*- and *m*-phenylene bridges,

Scheme 4. IR Stretching Frequencies ν_{CO} (cm^{-1}) of Isostructural trans-Coordinated Rhodiumcarbonyl Complexes of Trimethylphosphite, and Monodentate or Chelating Bis(imidazolio-diphenylphosphine) Ligands of 6, 5, and 7, Respectively

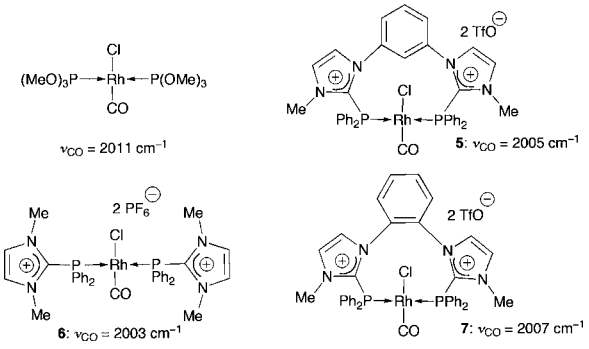

occurring in **7** and **5** respectively, have no influence on the donor ability of the imidazoliophosphine moieties, they can thus be considered as electronically insulating. Finally, while the trans-chelation observed in **7** could have been partly attributed to a steric repulsion between the closely facing N−Me groups,[12b] the same trans-coordination observed in the less constrained complex **5** (and all the more in **6**) is only attributed to a steric repulsion between the two donor ends of the ligands.

Having concluded that derivatives **4** and **5** would not proceed spontaneously to form the target pincer complex, the requisite metalation step was attempted by aiding the abstraction of the central proton (H1) of the *m*-phenylene ring in **5**. However, complex **5** remained impervious to all attempts using different bases (Et_3N, *n*-BuLi, *tert*-BuOK, NaH, AgOAc) and various conditions (solvents, temperature). Since H1 thus appeared less acidic than anticipated for such a dicationic complex, we undertook to abstract the chloride ligand, thereby increasing the overall positive charge of the complex.

Treating **5** with a stoichiometric amount of AgOTf in MeCN at room temperature, resulted in the formation of a white precipitate (AgCl). The ^{31}P NMR spectrum of the crude reaction mixture displayed a new signal at δ_p = +12.4 ppm (d, J_{PRh} = 127.6 Hz), which was attributed to the rhodium complex **8**, finally isolated in 94% yield (Scheme 5). Abstraction of the chloride ligand in **5** was also manifest in the new signals observed in ^{13}C

dx.doi.org/10.1021/ic3006508 | Inorg. Chem. 2013, 52, 48−58

Scheme 5. Sequential Formation of the Tricationic Bis(imidazoliophosphine) Complex 8 and Dicationic Diphosphinite Complex 9, from the Rhodium(I) Precursor 5

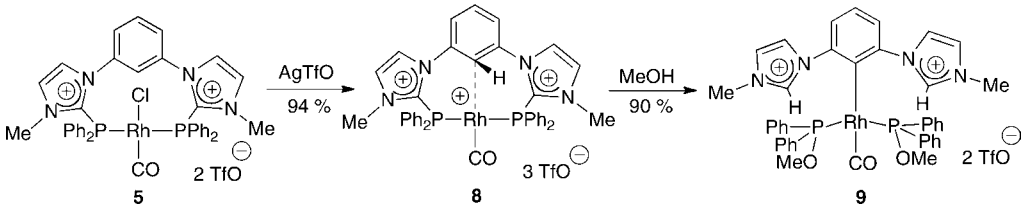

NMR (δ_{CO} = +187.7 ppm, broad d, J_{CRh} = 70.4 Hz) and IR (ν_{CO} = 2046 cm^{-1}) spectra of **8**, while its tricationic character (Scheme 5) was evidenced by ESI MS and HRMS data [m/z = 1037.0303 $(M - TfO^-)^+$]. That this new species is not the target PCP pincer complex was evident from the similar ^{31}P chemical shifts and J_{PRh} values of **5** and **8** (δ_p = +18.7 vs +12.4 ppm; J_{PRh} = 136 vs 128 Hz) which suggest only minor modifications in the electronic environment of the Rh(I) center.

The formal 14-electron count at the Rh(I) center in **8** obviously requires additional stabilization: this can be achieved by either labile coordination of a MeCN solvent molecule (as previously observed in a related tricationic rhodium complex),[12a] or intramolecular weak interaction of the Rh^+ center with the vicinal C1−H1 bond of the *m*-phenylene bridge of the ligand **3**. The latter scenario is supported by the observation of a broad deshielded ^1H NMR signal at +9.80 ppm, coupled to a ^{13}C nucleus in the aromatic region (δ_C = +111.4 ppm, broad s, in the $^{13}C-^1H$ HMQC spectrum). The width of the $^{13}C-^1H$ resonances is also consistent with a weak interaction with the ^{103}Rh nucleus ($J_{Rh,H}$ and $J_{Rh,C} \leq 5$ Hz). Since all attempts at growing high-quality single crystals of **8** were unsuccessful, the exact nature of the Rh···(C−H) interaction in this P(CH)P complex was investigated on the basis of theoretical calculations (see Section 2.2). The acronym "P(CH)P" is coined here for such conjugate acid precursors of classical PCP pincer complexes, the corresponding transformation formally consisting in oxidative addition and deprotonation.

The observed Rh···(C−H) interaction in tricationic **8** suggested that direct deprotonation of the C−H moiety might be possible. However, all attempts with various bases (Et_3N, *n*-BuLi, *tert*-BuOK, KHMDS, NaH, AgOAc) proved futile, and depending on the nature of the base, unreacted starting material or decomposition products were recovered. This paradoxical nonselective acidic behavior of the C−H bond in the vicinity of three formal positive charges is addressed by theoretical studies in Section 2.2. Multiple unsuccessful attempts at growing single crystals of **8** failed to allow unequivocal identification of this species. An unexpected transformation was observed during one such attempt when dry methanol was used as solvent. Monitoring the reaction by ^{31}P NMR spectroscopy at room temperature showed the complete disappearance of the signal of **8** (δ_p = +12.4 ppm, d, J_{PRh} = 127.6 Hz) after 12 h, and the concomitant emergence of a new signal at δ_p = +124.9 ppm (d, J_{PRh} = 143.8 Hz). The significantly different chemical shift of the new product indicates a major change in the chemical environment of the Rh center, but the key information for identifying the product was provided by ^{13}C NMR spectroscopy, which showed two quaternary carbon atoms resonating at low field as triplets of doublets: δ_C = +190.7 ppm (td, J_{CRh} = 57.9 Hz, J_{CP} = 16.3 Hz), δ_C = +177.0 ppm (td, J_{CRh} = 45.2 Hz, J_{CP} = 16.3 Hz). These ^{13}C chemical shifts were ultimately attributed to a remaining *C*O ligand and to the central sp^2-C1 atom of the *m*-phenylene bridge of the original ligand **3**, respectively. The presence of the CO ligand was further confirmed by IR spectroscopy (ν_{CO} = 2021 cm^{-1}). Finally, multinuclear 1D-2D NMR spectroscopy and mass spectroscopy [m/z = 951.1229 $(M - TfO^-)^+$] allowed the structure **9** to be assigned to the new product (Scheme 5), which could be isolated in 90% yield. Noteworthy, two sets of ^{13}C and ^1H NMR signals are observed for the N-methylimidazolium nuclei of **9** ($\delta(N_2CH)$ = 135.8 and 135.4 ppm, $\delta(N_2CH)$ = 9.59 and 9.51 ppm, $\delta(NCH)$ 36.8 and 36.7 ppm, $\delta(NCH)$ = 4.13 and 4.09 ppm): as other ^1H, ^{13}C, and ^{31}P signals are not split, this suggests diastereotopic conformational environments for the two imidazolium moieties (see Supporting Information).

Formation of the "open pincer" complex **9**, featuring a nonchelated aryl ligand is consistent with a nucleophilic displacement of the phosphenium centers from the NHC fragments by methanol molecules. A similar reactivity of chloride anions as alternative weak nucleophiles was indeed observed in [Pd(η^2-BIMIONAP)Cl_2], a complex of the BIMIONAP imidazoliophosphine ligand.[10c−e]

2.2. Theoretical Investigations. Geometries and NMR spectra of the initially targeted PCP pincer complex **10**, chlorinated precursor **5**, P(CH)P pincer complex **8**, and monodentate aryl complex **9** were calculated at the PCM-B3PW91/6-31G**/LANL2DZ*(Rh) level (Figure 3). The triflate counterions were not included in the calculations, but the acetonitrile solvent was implicitly accounted for as a dielectric continuum (ε = 35.688).

The calculation method is validated by a good agreement between the calculated C_s-symmetric structure of **5** and the corresponding XRD data (Table 1). As previously reported for related complexes at this calculation level,[10c] only the Rh−P and P−C bonds are found overestimated by about 0.05 Å. The Rh···C*i* distances (*i* = 1−3), ranging from 2.8 to 3.3 Å, are indicative of weak Rh-C*i* interactions: they are indeed significantly shorter than the corresponding sum of van der Waals radii (3.70 Å) but much longer than the sum of their covalent radii (2.10 Å).[18] The Rh···H1 distance of 2.85 Å (vs 2.78 Å from the XRD structure determination) is also slightly shorter than the corresponding sum of van der Waals radii (3.10 Å)[20] but the dominating Rh···(C1−H1) interaction is rather centered at the C1 atom. The calculated solution structure of **5** was further confirmed by the agreement between the experimentally measured ^{13}C, ^{31}P, and ^1H NMR chemical shifts and the ones calculated at the B3PW91/6-31+G**/LANL2DZ*(Rh) level on the static optimized geometries (see the Supporting Information, Table S1).

The calculated structure for **8**, which was obtained from chloride abstraction from **5**, deviates slightly from C_s-symmetry (Figure 3). The Rh···C*i* distances (*i* = 1−3) in **8** are significantly shortened (up to 0.30 Å for the Rh···C1 distance), whereas the C1−C2 and C1−C3 bonds of the *m*-phenylene ring are slightly

dx.doi.org/10.1021/ic3006508 | Inorg. Chem. 2013, 52, 48−58

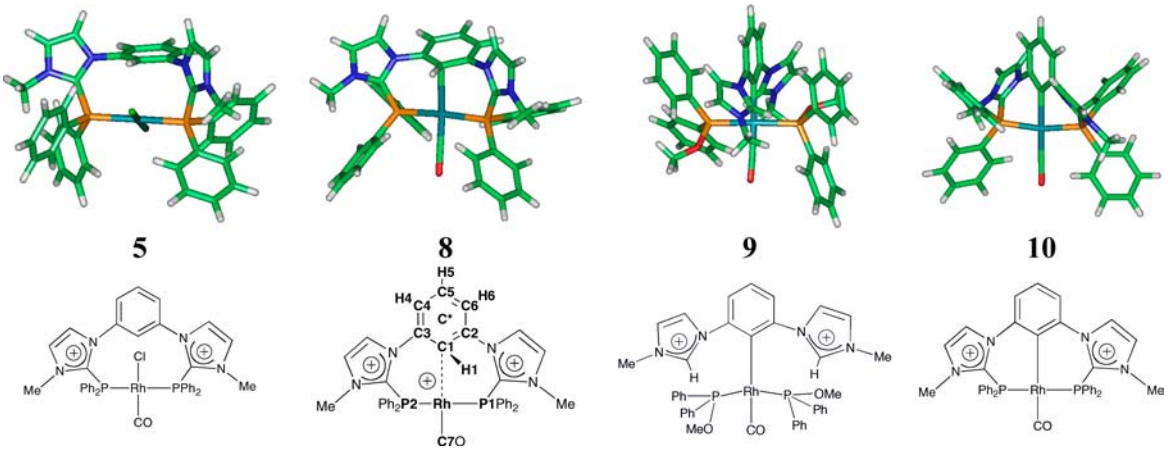

Figure 3. Calculated structures of the polycationic rhodium complexes **5** and **8**−**10** at the PCM-B3PW91/6-31G**/LANL2DZ*(Rh) level (acetonitrile solvent). Representative atom labeling is shown on complex **8**.

Table 1. Calculated vs Experimental Bond Distances (Å) and Angles (deg)[a] for the Complex Ions 5, 8−10 and Complexes A−B Shown in Scheme 6 (ref 19)[b]

	5		8	B	A	9	10
	calcd	exptl.	calcd	calcd	calcd	calcd	calcd
Rh−C1	2.813	2.766	2.516	2.514	2.256	2.114	2.117
Rh−H1	2.850	2.782	2.636	2.345	1.911		
Rh−C2	3.224	3.117	3.067			3.082	3.123
Rh−C3	3.304	3.299	3.056			3.166	3.123
Rh−C7	1.830	1.826	1.818	1.873	1.826	1.879	1.878
Rh−P1	2.351	2.300	2.362	2.382	2.340	2.362	2.311
Rh−P2	2.359	2.311	2.364	2.386	2.340	2.368	2.311
C1−C2	1.396	1.392	1.405			1.412	1.406
C1−C3	1.392	1.387	1.405			1.410	1.406
C1−H1	1.084		1.089	1.103	1.137		
C4−H4	1.086		1.084			1.085	1.085
C5−H5	1.084		1.084			1.085	1.085
C6−H6	1.078		1.078			1.084	1.084
Rh−H1−C1	77.1	79.4	71.8				
Rh−C1−H1	80.9	81.3	84.1				
Rh−C1−C2	93.9	90.9	99.0			126.8	123.6
Rh−C1−C3	97.8	99.8	98.5			120.6	123.6
C*−C1−H1	176.5	176.8	169.7		173.0		
C*−C5−H5	180.0	179.1	179.9			179.9	180.0
C1−C3−C4−C5	−0.1	−2.3	0.40		−1.73		
C1−C2−C6−C5	−1.6	0.9	−0.44		1.32		
P1−CN_2	1.840	1.856	1.840				1.845
P2−CN_2	1.847	1.859	1.843				1.845

[a]XRD data within esd errors. [b]Representative atom labelling as per complex **8** (Figure 3). Calculations performed at the B3PW91/6-31G**/LANL2DZ*(Rh) level.

elongated from 1.392 Å to 1.405 Å, thus revealing some increase in the π···Rh interaction (Table 1). The main structural change, however, is the bending of the C1−H1 bond by about 10° out of the plane of the *m*-phenylene ring. This data indicates a definite strengthening of the Rh···C1 interaction going from **5** to **8**, and complex **8** indeed appears as a P(CH)P pincer intermediate en route to the putative PCP pincer **10**. The optimized geometry of **10** was also calculated at the same level, and then compared to that of the experimentally obtained "open pincer" aryl complex **9** (a nonchelated version of **10**). Both **9** and **10** exhibit a C_2-symmetry optimized structure, with very similar Rh−C and Rh−P bond lengths (Table 1). Although no XRD analysis was available for **9** and **8** (see Section 2.1), their proposed structures are confirmed by the good agreement of the recorded ^{13}C, ^{31}P, and ^{1}H NMR data with the calculated ones at the B3PW91/6-31+G**/LANL2DZ*(Rh) level on the static optimized geometries (see the Supporting Information, Table S1). Initially, the C−H oxidative addition was anticipated to be the likely pathway for the formation of the PCP pincer complex **10** from **5**, but since this reaction could not be induced under many experimental conditions, the chemical bonding of the P(CH)P complex **8** was analyzed in detail to shed some light on this phenomenon.

The structural and NMR features of **8** are actually very similar to those of two related rhodium complexes described by Milstein et al. (Scheme 6):[19] (i) a η^2-C_{ipso},H agostic complex **A**, characterized experimentally, and (ii) a η^1-C_{ipso} intermediate **B**,

dx.doi.org/10.1021/ic3006508 | *Inorg. Chem.* 2013, 52, 48−58

Scheme 6. Structures of the Rhodium Complexes A and B Described by Milstein et al.[19]

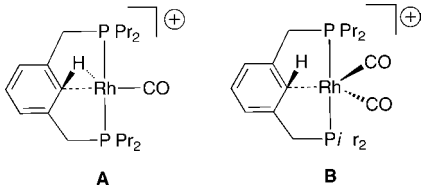

evidenced during computational investigations of the C−H oxidative addition pathway from **A**.

The so-called "agostic" 2c→1c* motifs refer to a T-shaped 3-center-2-electron interaction between a two-center donating bond (2c) and a one-center accepting orbital of a metal M (1c*) that tends toward bond scission through metal insertion or metallacycle formation as the interaction strengthens.[20] In η^2-C,H agostic complexes, the M···H distance generally ranges from 1.8 to 2.3 Å, whereas the M···H···C angle lies in the range 90−140°.[21] The structural features of complex **8** fall outside of these ranges, but are close to those of the η^1-C_{ipso} complex **B** (Table 1). This is further supported by a bonding overlap, involving a rhodium d orbital and a π orbital of the *m*-phenylene ring, that is visible in the canonical MO # 160, stabilized by 0.082 Ha (51.2 kcal/mol) below the highest occupied molecular orbital (HOMO; Figure 4).

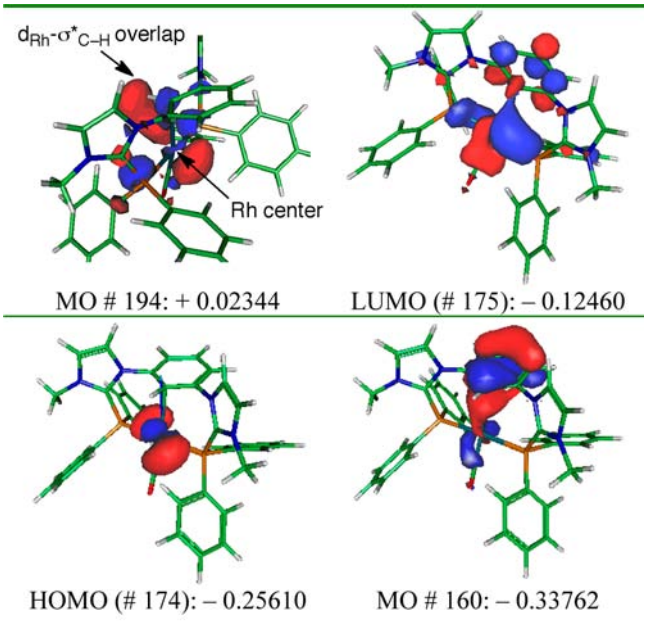

Figure 4. Selected molecular orbitals (MOs) of complex **8** featuring both the π-bonding overlap (MO # 160), and the d_{Rh}-σ^*_{C-H} preoxidative addition overlap (MO # 194). Calculations performed at the PCM-B3PW91/6-31G**/LANL2DZ*(Rh) level (acetonitrile solvent). Energies are given in hartree.

Natural Bond Orbital (NBO) analysis associated to agostic η^2-C,H interactions include the following main features:

(i) a noticeably depleted σ_{C-H} NBO, and a weak occupancy of the empty accepting metal orbital

(ii) a significant bond order for the M−H and M−C bonds as measured by Wiberg bond indices

(iii) a significant positive NBO atomic charge of the agostic hydrogen atom

(iv) a significant stabilization energy (>1.2 kcal/mol) of the interaction estimated via second order perturbation theory.[21]

The computed Wiberg bond indices of **8** are closer to those of the η^1-C_{ipso} complex **B** relative to those of the CH-agostic complex **A** (Scheme 6, Table 2). A weak interaction (1.78 kcal/mol)

Table 2. Wiberg Bond Indices Calculated at the B3PW91/6-31+G/DGDZVP(Rh)//B3PW91/6-31G**/LANL2DZ*(Rh) Level for 8 (Figure 3) and Complexes A−B Shown in Scheme 6 and Described in Ref 19**

	Rh−C1	Rh−H1	C1−H1	Rh−C7	C7−O
A	0.134	0.054	0.740	0.977	2.078
B	0.067	0.008	0.808	0.741	2.051
8	0.088	0.011	0.859	1.021	2.182

is revealed by the NBO donation $\sigma_{C1-H} \rightarrow$ LP*(Rh) where LP*(Rh) refers to the empty 5s orbital of the rhodium atom, is estimated from NBO analysis. With a population of 1.964, the σ_{C-H} is weakly depleted, whereas the empty 5s Rh orbital acquires a significant occupancy of 0.460. The latter value may, however, be related to stronger donor−acceptor interactions like π_{C1-C2}→LP*(Rh) (5.51 kcal/mol). Finally, it is noteworthy that the NBO atomic charge of H1 (+0.31) is comparable to that of the other aromatic hydrogen atoms (H4−H6) (+0.30).

All the NBO characteristics of complex **8** are thus consistent with a weak η^1-C1···Rh(I) interaction suggested by both structural data and MO analysis (see above). This interaction is formally analogous to the η^1-C bonding mode reported by Pregosin et al. in Ru(II) and Pd(II) complexes.[22]

Complex **8** might be considered as a stabilized intermediate on the way to the C−Rh−H oxidative addition process, which appears as a likely key step in the formation of the PCP "open pincer" complex **9**. This stabilization may be attributed to the strong electrophilic character of the Rh^+ center in **8**, and ultimately of the ligand **3**, preventing possible back-donation from a filled Rh d orbital into the C−H σ^* orbital. The latter overlap is found in MO # 194, lying 0.148 Ha (92.9 kcal/mol) above the lowest unoccupied molecular orbital (LUMO; Figure 4). Electron enrichment of the metal center is expected to lower the level of this empty orbital, and might thus be invoked as the driving force for the formation of **9** when methanol is used as a solvent. In accordance with the mechanism proposed for nucleophile-induced $[P-CN_2]^+$ bond cleavage,[10c] methanol molecules could indeed trigger such a cleavage in the highly electrophilic complex **8**. The latter would release a methyl diphenylphosphinite ligand, thus inducing an increase of the electronic density at the Rh(I) center, and favoring the C−H oxidative addition step (Scheme 7).

The electronic enrichment was first computationally envisaged through the coordination of the possibly released $Ph_2P(OMe)$ ligand in the putative complex **11** (Scheme 7). The corresponding two-component ligand "$Ph_2P(OMe)$ + monodentate imidazolium-imidazoliophosphine **3**′" derived from the methanolysis of **3** (Scheme 7) is indeed a priori globally more donating than the parent ligand **3** (acting in a pseudotridentate manner through the weak η^1-C coordination). This was indeed checked by calculation at the PBE/6-31G**/LANL2DZ*(Rh) level) of the average IR CO stretching frequencies in the corresponding $[RhL_2(CO)_2]^+$ complexes serving as probes in a general scale of the net electron-donating character of cis-coordinating ligands

dx.doi.org/10.1021/ic3006508 | Inorg. Chem. 2013, 52, 48−58

Scheme 7. Auxiliary Calculated Structures (See Text)

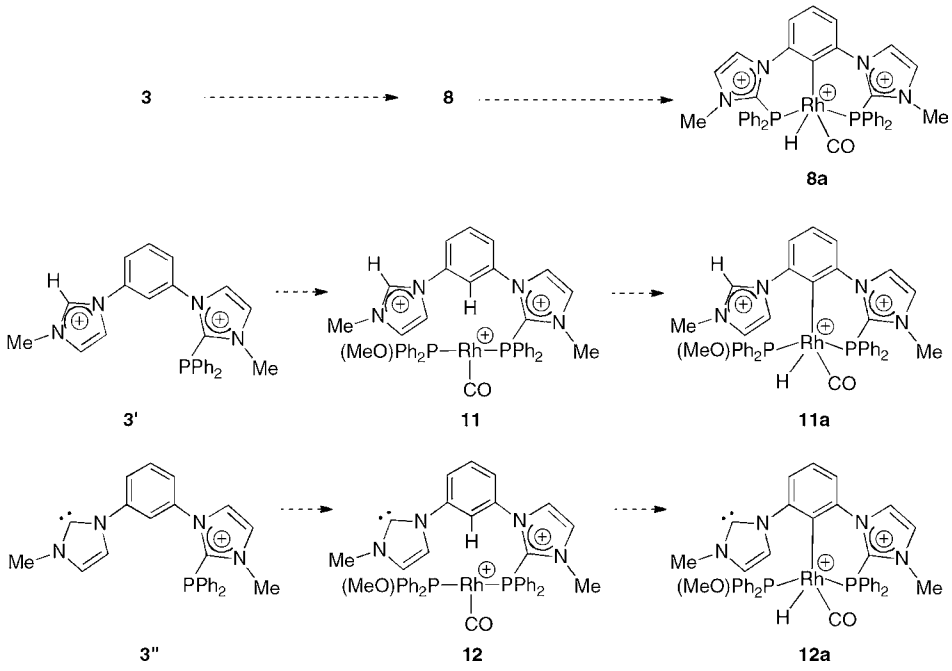

L_2:[15b] $\tilde{\nu}_{CO}([Rh(\mathbf{3})(CO)_2]^+)$ = 2080.2 cm^{-1} > $\tilde{\nu}_{CO}([Rh(\mathbf{3}')(Ph_2P(OMe))(CO)_2]^+)$ = 2074.4 cm^{-1} > $\tilde{\nu}_{CO}([Rh(Ph_2P(OMe))_2(CO)_2]^+)$ = 2072.6 cm^{-1}.

The Rh−C distance in complex **11** (4.031 Å) indicates the removal of the Rh−C interaction occurring in complex **8** (2.516 Å) that was a priori expected to facilitate the oxidative addition process. The energy profiles of the oxidative addition pathways from **8** and **11** to their respective C−H oxidative adducts **8a** and **11a** (Scheme 7) are shown in Figure 5, and the calculated

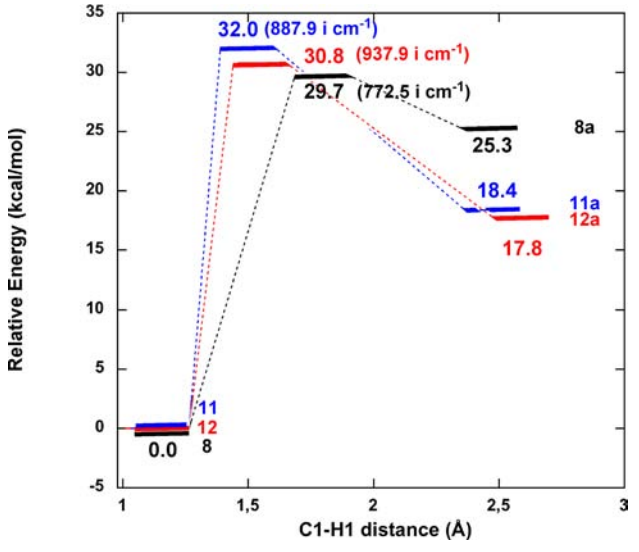

Figure 5. Oxidative addition energy profiles from the complexes **8** (*in black*), **11** (*in blue*), and **12** (*in red*) to the respective C−H oxidative adducts **8a**, **11a**, and **12a** (Scheme 7). Calculations performed at the PCM-B3PW91/6-31G**/LANL2DZ*(Rh) level (acetonitrile solvent). Relative energies, given in kcal/mol, are not corrected for zero-point energy.

structures of the corresponding transition states and oxidative addition products are given in the Supporting Information, Figure S1. With respect to **11** and **8**, the $Ph_2P(OMe)$-Rh-enriched adduct **11a** was thus found more stabilized than **8a**, both of them exhibiting square-pyramidal structures (18.4 kcal/mol vs 25.3 kcal/mol). Conversely, the kinetic barrier for the transformation **11**→**11a** (32.0 kcal/mol) was found to be higher than the corresponding barrier for **8**→**8a** (29.7 kcal/mol), and in accordance with the Hammond postulate, **8aTS** is a later transition state (C1···H1 = 1.555 Å) than **11aTS** (C1···H1 = 1.519 Å).

The reaction barrier is thus increased upon electronic enrichment of the Rh center by the $Ph_2P(OMe)$ ligand in **11**, while preserving the dicationic character of the ligand **3** of **8** in the ligand **3′** containing the C−H bond to be activated in **11**.

In spite of the protic experimental conditions (methanol is used as the solvent), the methanolysis of the trication **8** might proceed sequentially through a transient dicationic complex **12** of the ligand **3′′** (Scheme 7) bearing a pendent imidazolylidene moiety that could deprotonate the CH vertex either directly or via the C−H oxidative adduct **12a**. The latter is found to be relatively more stabilized (by 17.8 kcal/mol vs **12**) than **8a** (25.3 kcal/mol vs **8**), but less than **11a** (18.4 kcal/mol vs **11**, Figure 5). The corresponding kinetic barrier through the transition state **12aTS** was however found slightly higher (30.8 kcal/mol) than that of the **8**→**8a** process. The **12**→**12a** barrier is also found to be lower than the **11**→**11a** barrier, in accordance with the concomitant electronic enrichment of the monocationic ligand **3′′** with respect to the dicationic ligand **3′**.

The effect of electron enrichment was utimately investigated in the $[Rh(CO)(PMe_3)_2(C_6H_6)]^+$ model complex where the dicationic diphosphine **3** is substituted by two strongly electron-donating PMe_3 ligands, but instead of the C1−H1 activation, only an η^2-arene Rh(I) complex was obtained (Supporting Information, Figure S2). These findings are therefore not in favor of a C−H oxidative addition pathway for the formation of the "open pincer" complex **9**.

Keeping in mind that the medium of the formation of **9** is very weakly basic, two alternative mechanisms could be envisaged from the η^1-C rhodium complex **8**. The reacting MeOH molecule may indeed first coordinate to the Rh center (Scheme 8, route a)

dx.doi.org/10.1021/ic3006508 | *Inorg. Chem.* 2013, 52, 48−58

Scheme 8. Possible Mechanisms for the Formation of the "Open Pincer" Complex 9 from the Precursor 8 in the Presence of Methanol, Consistent with the Absence of Strong Base

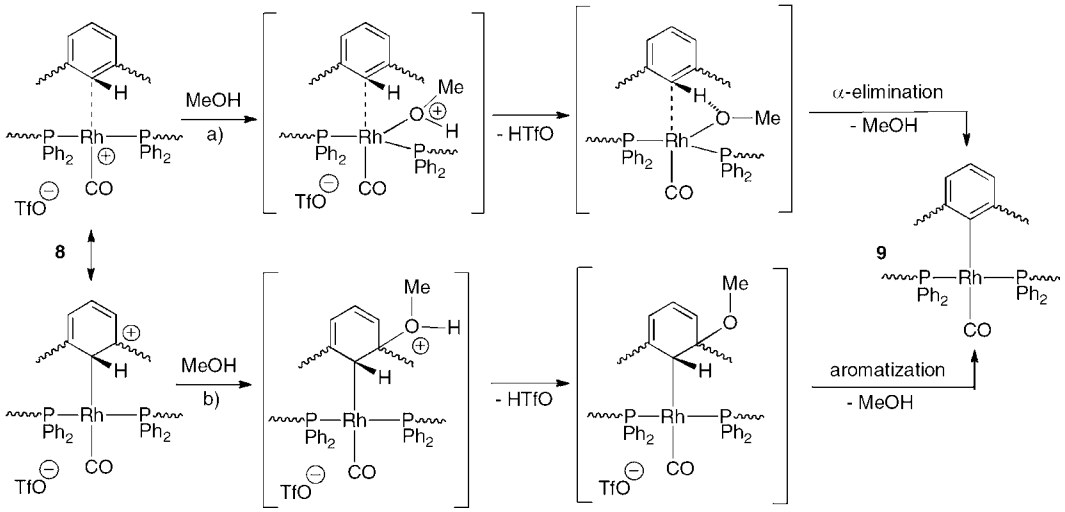

or add to the central phenylene ring by nucleophilic attack on the activated α-positions of the C1 carbon atom (Scheme 8, route b; Mulliken charges at C2 and C3: + 0.12. See Figure 3 for labeling). In both cases, the resulting highly acidic oxonium would then be deprotonated by the weakly basic TfO^- anion. In route a, an α-elimination process (in the "organometallic sense") would ensue from the proximity of the Rh-coordinated methoxy oxygen atom and the phenylene H1-atom, thus leading to formation of the "open pincer" **9**.[23] In route b, β-elimination of methanol (in the "organic sense") would be dictated by the phenylene rearomatization driving force.

3. CONCLUSION

The use of the chelating and highly electron-poor bis(imidazoliophosphine) ligand **3** allowed to generate the Rh(I) complexes **5**, **8**, and **9**, that exhibit unprecedented structural features. Complex **8** appears as a η^1-C P(CH)P pincer intermediate that is poised to form the putative PCP pincer complex **10**. Although the nature of the bonding in complex **8**, calling for the contribution of a C-hypervalent Lewis structure in Scheme 5, deserves further theoretical investigations, the long debated C−H oxidative pathway in the formation of classical PCP pincer complexes could be ruled out in the present case on the basis of DFT calculation results. The inescapable findings of the computational investigations suggest two alternative mechanisms based on classical organometallic or organic key-processes (α-elimination and aromaticity-driven β-elimination) and consistent with the absence of strong base in the medium. Through the formation of the aryl-Rh "open pincer" complex **9**, the electrophilic reactivity of the P−CN_2 bond in the imidazoliophosphine ligands is shown to open new perspectives in the investigation of selective reorganization processes within the coordination sphere of transition metals such as Rh(I) centers. Given the now demonstrated unique coordination properties for the *ortho*- and *meta*-phenylene-bis(imidazoliophosphine) ligands, efforts towards the comparative study of the *para*-phenylene-bis(imidazoliophosphine) isomers deserve to be undertaken shortly.

EXPERIMENTAL SECTION

General Remarks. THF, diethyl ether, and toluene were dried and distilled over sodium/benzophenone, while pentane, dichloromethane, acetonitrile, and methanol were dried over CaH_2. All other reagents were used as received from commercial sources. All reactions were carried out under an argon atmosphere, using Schlenk and vacuum line techniques. The following analytical instruments were used. ^{1}H, ^{13}C, and ^{31}P NMR: Bruker ARX 250, DPX 300, and Avance 500. NMR chemical shifts δ are in ppm, with positive values to high frequency relative to the tetramethylsilane reference for ^{1}H and ^{13}C, and to the H_3PO_4 reference for ^{31}P; coupling constants J are in hertz (Hz). ^{103}Rh chemical shifts are given to high frequency from $\Xi(^{103}Rh) = 3.16$ MHz. Elemental analyses: Perkin-Elmer CHN 2400.

2-(Diphenylphosphanyl)-1-{3-[2-(diphenylphosphanyl)-1*H*-imidazol-1-yl]phenyl}-1*H*-imidazole (2). To a solution of 1,3-bis(N-imidazolyl)benzene **1** (500 mg, 2.38 mmol) in THF (50 mL) cooled to −78 °C was added *n*-butyllithium (2.5 M in hexane, 2.0 mL, 5.0 mmol). The suspension was then warmed to −20 °C and stirred for 2 h. After addition of chlorodiphenylphosphine (0.93 mL, 5.0 mmol) at −20 °C, the solution was stirred at room temperature for 12 h. After evaporation of the solvent under vacuum, purification by chromatography on silica gel (CH_2Cl_2/pentane) of the residue gave **2** as a white solid (1.15 g, 83%). Recrystallization at −20 °C from CH_2Cl_2/toluene afforded **2** as white crystals (mp 58−59 °C).

^{1}H NMR ($CDCl_3$, 25 °C): δ = 7.28−7.50 (m, 25H, H_{ar}), 7.18 (brs, 2H, H_{ar}), 7.10 (brs, 1H, H_{ar}). ^{13}C NMR ($CDCl_3$, 25 °C): δ = 146.9 (d, J_{CP} = 8.6, C), 138.4 (s, C), 135.0 (d, J_{CP} = 5.1, C), 133.9 (d, J_{CP} = 20.8, CH_{ar}), 131.6 (s, CH_{ar}), 129.6 (s, CH_{ar}), 129.3 (s, CH_{ar}), 128.6 (d, J_{CP} = 7.9, CH_{ar}), 128.2 (d, J_{CP} = 4.8, CH_{ar}), 124.2 (t, J_{CP} = 3.3, CH_{ar}), 123.6 (s, CH_{ar}). ^{31}P NMR ($CDCl_3$, 25 °C): δ = −28.4. MS (ESI+): m/z = 579.2 $[M + H]^+$; HRMS (ESI+): calcd. for $C_{36}H_{29}N_4P_2$ 579.1867; found, 579.1880. Elemental analysis, calcd (%) for $C_{36}H_{28}N_4P_2$: C 74.73, H 4.88, N 9.68; found: C 73.93, H 4.98, N 9.29.

2-(Diphenylphosphanyl)-1-{3-[2-(diphenylphosphanyl)-3-methyl-1*H*-imidazol-3-ium-1 yl]phenyl}-3-methyl-1*H*-imidazol-3-ium bistriflate (3). To a solution of **2** (1.10 g, 1.90 mmol) in CH_2Cl_2 (40 mL) cooled at −78 °C was added methyl-trifluoromethanesulfonate (0.42 mL, 3.80 mmol). The solution was warmed to room temperature and stirred for 2 h. After evaporation of the solvent under vacuum, the residue was washed with Et_2O (40 mL), affording a white solid (1.64 g, 95%). Recrystallization at −20 °C from MeCN/Et_2O afforded **3** as white crystals (mp: 56−57 °C).

^{1}H NMR (CD_3CN, 25 °C): δ = 7.83 (brs, 2H, H_{ar}), 7.72 (brs, 2H, H_{ar}), 7.52−7.30 (m, 24H, H_{ar}), 3.52 (s, 6H, NCH_3). ^{13}C NMR (CD_3CN, 25 °C): δ = 144.7 (d, J_{CP} = 58.3, C), 135.8 (s, C), 133.4 (d, J_{CP} = 21.6, CH_{ar}), 131.0 (s, CH_{ar}), 129.8 (d, J_{CP} = 7.8, CH_{ar}), 129.5 (s, CH_{ar}), 129.0 (s, CH_{ar}), 128.3 (s, CH_{ar}), 127.8 (s, C), 126.8 (s, CH_{ar}), 125.8 (t, J_{CP} = 2.6, CH_{ar}), 125.3 (s, CH_{ar}), 121.2 (q, J_{CF} = 320.8, CF_3SO_3), 37.8 (CH_3). ^{31}P NMR (CD_3CN, 25 °C):δ = −21.1. MS(ES+): m/z: 757.2 $[M - CF_3SO_3^-]^+$; HRMS(ES+) calcd for $C_{39}H_{34}N_4O_3F_3P_2S$, 757.1779; found, 757.1785. Elemental analysis, calcd (%) for

dx.doi.org/10.1021/ic3006508 | *Inorg. Chem.* 2013, 52, 48−58

$C_{40}H_{34}F_6N_4O_6P_2S_2$: C 52.98, H 3.78, N 6.18; found: C 51.92, H 3.83, N 5.85.

Rhodium(I) Chloride Complexes of the Ligand 3 (4, 5). A mixture of $[RhCl(cod)]_2$ (163 mg, 0.33 mmol) and dication **3** (500 mg, 0.55 mmol) was dissolved in CH_2Cl_2 (20 mL) at −40 °C, and stirred at room temperature for 12 h. After evaporation of the solvent, the crude residue was washed with Et_2O (30 mL) affording **4** as a yellow powder (572 mg, 90%; mp 216−218 °C). Then complex **4** was dissolved in CH_2Cl_2 (10 mL), and carbon monoxide was bubbled for 30 min at room temperature. After evaporation of the solvent, and washing with Et_2O (20 mL), **5** was obtained as a yellow powder (404 mg, 76%). Recrystallization from MeCN/Et_2O at 0 °C afforded **5** as orange crystals (mp 112−113 °C).

RhCl(cod)[3] Complex (4). ^{1}H NMR ($CDCl_3$, 25 °C): δ = 7.77−7.16 (m, 28H, H_{ar}), 5.70 (br, 2H, CH_{cod}), 4.55 (br, 2H, CH_{cod}), 3.71 (s, 6H, NCH_3), 2.43 (brs, 4H, CH_{2cod}), 2.14 (brs, 4H, CH_{2cod}). ^{13}C NMR ($CDCl_3$, 25 °C): δ = 140.9 (d, J_{CP} = 23.6, C), 135.3 (s, C), 132.9 (s, CH_{ar}), 130.1 (s, CH_{ar}), 129.8 (s, CH_{ar}), 128.8−124.5 (m, C, CH_{ar}), 120.7 (q, J_{CF} = 320.8, CF_3SO_3), 107.8 (s, CH_{cod}), 73.0 (br, CH_{cod}), 39.5 (CH_3), 32.8 (s, CH_{2cod}), 28.7 (s, CH_{2cod}). ^{31}P NMR ($CDCl_3$, 25 °C): δ = +26.4 (d, J_{PRh} = 150.4). ^{103}Rh NMR ($CDCl_3$, 25 °C): δ = +379 ppm. MS(ES+): m/z 1003.1 $[M\text{-}CF_3SO_3^-]^+$; HRMS(ES+) calcd for $C_{47}H_{46}ClN_4O_3F_3P_2SRh$: 1003.1462; found: 1003.1458.

RhCl(CO)[3] Complex (5). ^{1}H NMR (CD_3CN, 25 °C): δ = 8.70 (s, 1H, H_{ar}), 8.10 (d, 2H, J_{HH} = 5.0, H_{ar}), 7.87 (d, 2H, J_{HH} = 5.0, H_{ar}), 7.83−7.42 (m, 23H, H_{ar}), 3.30 (s, 6H, NCH_3). ^{13}C NMR (CD_3CN, 25 °C): δ = 182.9 (td, J_{CRh} = 74.2, J_{CP} = 15.1, CO), 140.6 (t, J = 13.8, C), 135.4 (s, CH_{ar}), 134.8 (s, C), 133.0 (s, CH_{ar}), 132.7 (d, J_{CP} = 6.3, CH_{ar}), 132.6 (d, J_{CP} = 6.3, CH_{ar}), 130.0 (s, CH_{ar}), 129.8 (t, J_{CP} = 5.0, CH_{ar}), 129.6 (s, CH_{ar}), 129.3 (t, J_{CP} = 5.0, CH_{ar}), 129.1 (s, CH_{ar}), 127.7 (s, CH_{ar}), 126.7 (t, J_{CP} = 25.8, C), 124.8 (s, CH_{ar}), 122.9 (t, J_{CP} = 23.2 C), 121.1 (q, J_{CF} = 320.8, CF_3SO_3), 39.2 (CH_3). ^{31}P NMR (CD_3CN, 25 °C): δ = +18.7 (d, J_{PRh} = 135.7). ^{103}Rh NMR (CD_3CN, 25 °C): δ = −75 ppm. MS(ES+): m/z 923.0 $[M - CF_3SO_3^-]^+$; HRMS(ES+) calcd for $C_{40}H_{34}N_4O_4F_3P_2SClRh$, 923.0472; found, 923.0491. Elemental analysis, calcd (%) for $C_{41}H_{34}ClF_6N_4O_7P_2RhS_2$: C 45.89, H 3.19, N 5.22; found: C 45.00, H 3.20, N 5.10.

Rhodium(I)carbonyl Triflate Complex of the Ligand 3 (8). A mixture of **5** (280 mg, 0.26 mmol) and silver trifluoromethanesulfonate (74 mg, 0.29 mmol) cooled to −20 °C, was dissolved in MeCN (10 mL). After warming up to room temperature, the solution was stirred for 12 h. The solid was then filtered off, and the solution evaporated under vacuum. After addition of THF (10 mL) and filtration of the remaining solid, the solvent was removed under vacuum, affording **8** as a yellow solid (291 mg, 94%).

^{1}H NMR (CD_3CN, 25 °C): δ = 9.81 (br, 1H, H_{ar}), 8.26 (s, 2H, H_{ar}), 8.05 (s, 2H, H_{ar}), 7.77−7.38 (m, 23H, H_{ar}), 3.28 (s, 6H, NCH_3). ^{13}C NMR (CD_3CN, 25 °C): δ = 187.7 (d, J_{CRh} = 70.4, CO), 138.5 (peudo-t, J = 17.6, C), 135.9 (d, J = 46.5, C), 135.5 (s, C), 133.4 (s, CH_{ar}), 133.1 (s, CH_{ar}), 132.0 (s, CH_{ar}), 131.7 (s, CH_{ar}), 130.8 (s, CH_{ar}), 130.4−130.3 (m, CH_{ar}), 129.5 (s, CH_{ar}), 124.3 (br, C), 121.0 (q, J_{CF} = 320.8, CF_3SO_3), 120.8 (br, C), 111.4 (s, CH_{ar}), 39.4 (CH_3). ^{31}P NMR (CD_3CN, 25 °C):δ = +12.4 (d, J_{PRh} = 125.6). ^{103}Rh NMR (CD_3CN, 25 °C): δ = −138 ppm. MS(ES+):m/z 1037.0 $[M - CF_3SO_3^-]^+$; HRMS(ES+) calcd for $C_{41}H_{34}N_4O_7F_6P_2RhS_2$, 1037.0303; found, 1037.0319. Elemental analysis, calcd (%) for $C_{42}H_{34}F_9N_4O_{10}P_2RhS_3$: C 42.51, H 2.89, N 4.72; found: C 37.90, H 2.84, N 4.76 (the low value found for the carbon element might be due to residual silver).

Rhodium(I)carbonyl Aryl Complex 9. Complex **8** (80 mg, 0.067 mmol) was dissolved in dry methanol (2 mL). After stirring overnight at room temperature, the solvent was then removed under vacuum. After washing by Et_2O (10 mL), **9** was obtained as a brown solid (67 mg, 90%).

^{1}H NMR (CD_2Cl_2, 25 °C): 9.59 (s, 1H, CH), 9.51 (s, 1H, CH), 8.35 (d, 1H, J_{HH} = 5.0, H_{ar}), 8.11 (s, 1H, H_{ar}), 7.93 (brs, 2H, H_{ar}), 7.82−7.71 (m, 4H, H_{ar}), 7.65−7.63 (m, 3H, H_{ar}), 7.59−7.41 (m, 15H, H_{ar}), 6.84 (d, 1H, J_{HH} = 1.9, H_{ar}), 4.13 (s, 3H, CH_3N), 4.09 (s, 3H, CH_3N), 3.47 (s, 6H, CH_3O). ^{13}C NMR (CD_2Cl_2, 25 °C): δ = 190.7 (td, J_{CRh} = 57.8, J_{CP} = 16.3, CO), 177.0 (td, J_{CRh} = 44.0, J_{CP} = 17.6, C), 140.0 (s, C), 135.9 (s, C), 135.8 (broad s, N_2CH), 135.4 (broad s, N_2CH), 135.3 (s, C), 133.6 (t, J_{CP} = 23.9, C), 133.5 (t, J_{CP} = 23.9, C), 132.7 (s, CH_{ar}), 132.0 (s, CH_{ar}), 131.9 (s, CH_{ar}), 131.7 (s, CH_{ar}), 131.6 (d, J_{CP} = 7.5, CH_{ar}), 131.1 (t, J_{CP} = 6.3, CH_{ar}), 130.8 (s, CH_{ar}), 129.1 (t, J_{CP} = 5.0, CH_{ar}), 128.9 (t, J_{CP} = 5.0, CH_{ar}), 128.8 (s, CH_{ar}), 124.9 (s, CH_{ar}), 124.8 (s, CH_{ar}), 124.5 (s, CH_{ar}), 123.3 (s, CH_{ar}), 123.2 (s, CH_{ar}), 123.1 (s, CH_{ar}), 121.6 (s, CH_{ar}), 121.4 (s, CH_{ar}), 120.8 (q, J_{CF} = 321.8, CF_3SO_3), 55.0 (s, CH_3O), 36.8 (s, CH_3N), 36.7 (s, CH_3N). ^{31}P NMR (CD_2Cl_2, 25 °C):δ = +124.9 (d, J_{PRh} = 143.8). ^{103}Rh NMR (CD_3CN, 25 °C): δ = −255 ppm. MS(ES+): m/z 951.1 $[M - CF_3SO_3^-]^+$; HRMS(ES+) calcd for $C_{42}H_{41}N_4O_6F_3P_2SRh$, 951.1229; found, 951.1255. Elemental analysis, calcd (%) for $C_{43}H_{41}F_6N_4O_9P_2RhS_2$: C 46.92, H 3.75, N 5.09; found: C 45.62, H 3.27, N 5.07.

Crystal Structure Determination of Compounds 2, 3, and 5. Intensity data for compounds **2**, **3**, and **5** were collected at 180 K on an Apex2 Bruker diffractometer using a graphite-monochromated Mo Kα radiation source and equipped with an Oxford Cryosystems Cryostream Cooler Device. Structures were solved using SIR92[24] or SUPERFLIP,[25] and refined by full-matrix least-squares procedures on F using the programs of the PC version of CRYSTALS.[26] Atomic scattering factors were taken from the International tables for X-ray Crystallography.[27] All non-hydrogen atoms were refined anisotropically. Hydrogen atoms were refined using a riding model. Absorption corrections were introduced using the program MULTISCAN.[28] For **3**, the crystal was of poor quality (a phenyl group is disordered). Refinement of the used model led to a satisfactory solution with a 0.5:0.5 occupancy ratio. It was not possible to resolve diffuse electron-density residuals (enclosed solvent molecules). Finally, treatment with the SQUEEZE[29] facility from PLATON[30] resulted in a better refinement.

Crystal data for **2**: $C_{36}H_{28}N_4P_2$, M = 578.59 g·mol^{-1}, Monoclinic, a = 10.1714(8), b = 20.5363(13), c = 15.1935(9) Å, β = 109.556(3)°, V = 2990.6(4) Å^3, T = 180 K, space group $P2_1/c$, Z = 4, μ(Mo-Kα) = 0.178 mm^{-1}, 33195 reflections measured, 7769 unique (R_{int} =0.043), 5067 reflections used in the calculations $[I > 3\sigma(I)]$, 379 parameters, R1 = 0.0418, wR2 = 0.0446.

Crystal data for **3**: $C_{40}H_{34}F_6N_4O_6P_2S_2$, M = 906.80 g·mol^{-1}, monoclinic, a = 15.633(3), b = 22.942(5), c = 14.911(3) Å, β = 116.15(3)°, V = 4800(2) Å^3, T = 180 K, space group $C2/c$, Z = 4, μ(Mo-Kα) = 0.246 mm^{-1}, 22578 reflections measured, 7462 unique (R_{int} =0.0659), 4905 reflections used in the calculations $[I > 3\sigma(I)]$, 266 parameters, R1 = 0.1134, wR2 = 0.1073.

Crystal data for **5**: $C_{41}H_{34}ClF_6N_4O_7P_2RhS_2$, M = 1073.17 g·mol^{-1}, triclinic, a = 12.7519(12), b = 13.7106(13), c = 13.8297(13) Å, α = 77.390(4), β = 79.713(4), γ = 68.869(4)°, V = 2187.7(4) Å^3, T = 180 K, space group $P\bar{1}$, Z = 2, μ(Mo-Kα) = 0.700 mm^{-1}, 55848 reflections measured, 13792 unique (R_{int} = 0.021), 11019 reflections used in the calculations $[I > 3\sigma(I)]$, 577 parameters, R1 = 0.0299, wR2 = 0.0306.

COMPUTATIONAL DETAILS

Geometries were fully optimized at the PCM-B3PW91/6-31G**/LANL2DZ*(Rh) level of calculation using Gaussian09.[31] LANL2DZ*(Rh) means that f-polarization functions derived by Ehlers et al.[32] for Rh have been added to the LANL2DZ(Rh) basis set. Vibrational analysis was performed at the same level as the geometry optimization. Solvent effects were included using the polarizable continuum model (PCM) implemented in Gaussian09 for acetonitrile (ε = 35.688). From these optimized structures, the potential energy surface was explored along the reaction coordinate (C1−H1 distance) at the same calculation level. The intrinsic reaction coordinate was followed using the IRC technique implemented in Gaussian 09 for all located transition states.

The magnetic shielding tensor was calculated at the B3PW91/6-31+G**/LANL2DZ*(Rh) using the GIAO (gauge-independent atomic orbital) method implemented in Gaussian09.[31] The ^{31}P NMR chemical shifts were estimated with respect to the usual H_3PO_4 reference.

NBO analysis[33] was performed using NBO 5.G.[34] In NBO analysis, deviations from idealized Lewis structures are interpreted in terms of donor−acceptor interactions between filled localized bonds or lone-pairs (donors) and empty antibonds (acceptors). They are referred to as "delocalization" corrections to the zeroth-order natural Lewis structure and estimated by the second-order perturbation theory. The stabilization

dx.doi.org/10.1021/ic3006508 | Inorg. Chem. 2013, 52, 48−58

energy $E^{(2)}$ associated with delocalization is given by $E^{(2)} = n\langle F_{ij}\rangle^2/\varepsilon_{ij}$, where F_{ij} is the off-diagonal NBO Fock matrix element (and can be taken as proportional to the overlap between those orbitals), ε_{ij} is the energy difference between the donor NBO i and the acceptor NBO j, and n is the occupancy of the NBO i. Since perturbation theory is valid for small perturbations only, absolute stabilizations become less reliable as their value increase. General trends are therefore more meaningfull than the absolute values of the energetic contributions. Molecular orbitals were plotted using the GABEDIT program.[35]

■ ASSOCIATED CONTENT

Supporting Information

Complementary calculation details are available from the authors. Crystallographic data is provided in CIF format. ^{1}H, and ^{31}P NMR spectra are also provided. This material is available free of charge via the Internet at http://pubs.acs.org.

■ AUTHOR INFORMATION

Corresponding Author

*Fax: (+33)5 61 55 30 03. E-mail: yves.canac@lcc-toulouse.fr (Y.C.), chauvin@lcc-toulouse.fr (R.C.).

Notes

The authors declare no competing financial interest.

■ ACKNOWLEDGMENTS

In addition to thanking the Ministère de l'Enseignement Supérieur de la Recherche et de la Technologie and the Université Paul-Sabatier, the authors thank also the Centre National de la Recherche Scientifique, and the ANR program (ANR-08-JCJC-0137-01). The theoretical studies were performed using HPC resources from CALMIP (Grant 2011 [0851]), and from GENCI-[CINES/IDRIS] (Grant 2011 [085008]).

■ REFERENCES

(1) (a) Albrecht, M.; van Koten, G. *Angew. Chem., Int. Ed.* **2001**, *40*, 3750. (b) Lagt, M. Q.; van Zwieten, D. A. P.; Moerkerk, A. J. C. M.; Gebbink, R. J. M. K.; van Koten, G. *Coord. Chem. Rev.* **2004**, *248*, 2275. (c) Nishiyama, H. *Chem. Soc. Rev.* **2007**, *36*, 1133. (d) Morales-Morales, D.; Jensen, C. M. *The Chemistry of Pincer Compounds*; Elsevier: Amsterdam, The Netherlands, 2007. (e) Morales-Morales, D. *Mini-Rev. Org. Chem.* **2008**, *5*, 141. (f) Benito-Garagorri, D.; Kirchner, K. *Acc. Chem. Res.* **2008**, *41*, 201. (g) Selander, N.; Szabó, K. J. *Chem. Rev.* **2011**, *111*, 2048.

(2) (a) Rybtchinski, B.; Milstein, D. *Angew. Chem., Int. Ed.* **1999**, *28*, 870. (b) van der Boom, M. E.; Milstein, D. *Chem. Rev.* **2003**, *103*, 1759.

(3) (a) Adams, J. J.; Lau, A.; Arulsamy, N.; Roddick, D. M. *Inorg. Chem.* **2007**, *46*, 11328. (b) Adams, J. J.; Lau, A.; Arulsamy, N.; Roddick, D. M. *Organometallics* **2011**, *30*, 689. (c) Adams, J. J.; Arulsamy, N.; Roddick, D. M. *Organometallics* **2011**, *30*, 697.

(4) Chase, P. A.; Gagliardo, M.; Lutz, M.; Spek, A. L.; van Klink, G. P. M.; van Koten, G. *Organometallics* **2005**, *24*, 2016.

(5) (a) Kossoy, E.; Iron, M. A.; Rybtchinski, B.; Yehoshoa, B. D.; Shimon, L. J. W.; Konstantinovski, L.; Martin, J. M. L.; Milstein, D. *Chem.—Eur. J.* **2005**, *11*, 2319. (b) Kossoy, E.; Rybtchinski, B.; Diskin-Posner, Y.; Shimon, L. J. W.; Leitus, G.; Milstein, D. *Organometallics* **2009**, *28*, 523.

(6) (a) Rubio, M.; Suárez, A.; del Río, D.; Galindo, A.; Álvarez, E.; Pizzano, A. *Dalton Trans.* **2007**, 407. (b) Rubio, M.; Suárez, A.; del Río, D.; Galindo, A.; Álvarez, E.; Pizzano, A. *Organometallics* **2009**, *28*, 547.

(7) (a) Li, J.; Lutz, M.; Spek, A. L.; van Klink, G. P. M.; van Koten, G.; Gebbink, R. J. M. *Organometallics* **2010**, *29*, 1379. (b) Niu, J. L.; Hao, X. Q.; Gong, J. F.; Song, M. P. *Dalton Trans.* **2011**, *40*, 5135.

(8) (a) Morales-Morales, D.; Redón, R.; Yung, C.; Jensen, C. M. *Chem. Commun.* **2000**, 1619. (b) Salah, A. B.; Zargarian, D. *Dalton Trans.* **2011**, *40*, 8977.

(9) (a) Scholl, M.; Ding, S.; Lee, C. W.; Grubbs, R. H. *Org. Lett.* **1999**, *1*, 953. (b) Debono, N.; Canac, Y.; Duhayon, C.; Chauvin, R. *Eur. J. Inorg. Chem.* **2008**, 2991. (c) Abdellah, I.; Debono, N.; Canac, Y.; Vendier, L.; Chauvin, R. *Chem.—Asian. J.* **2010**, *5*, 1225.

(10) (a) Kuhn, N.; Fahl, J.; Bläser, D.; Boese, R. *Z. Anorg. Allg. Chem.* **1999**, *625*, 729. (b) Azouri, M.; Andrieu, J.; Picquet, M.; Richard, P.; Hanquet, B.; Tkatchenko, I. *Eur. J. Inorg. Chem.* **2007**, 4877. (c) Abdellah, I.; Lepetit, C.; Canac, Y.; Duhayon, C.; Chauvin, R. *Chem.—Eur. J.* **2010**, *16*, 13095. (d) Abdellah, I.; Boggio-Pasua, M.; Canac, Y.; Lepetit, C.; Duhayon, C.; Chauvin, R. *Chem.—Eur. J.* **2011**, *17*, 5110. (e) Maaliki, C.; Lepetit, C.; Canac, Y.; Bijani, C.; Duhayon, C.; Chauvin, R. *Chem.—Eur. J.* **2012**, *18*, 7705.

(11) For a recent review: Canac, Y.; Maaliki, C.; Abdellah, I.; Chauvin, R. *New. J. Chem.* **2012**, *36*, 17.

(12) (a) Canac, Y.; Debono, N.; Vendier, L.; Chauvin, R. *Inorg. Chem.* **2009**, *48*, 5562. (b) Canac, Y.; Debono, N.; Lepetit, C.; Duhayon, C.; Chauvin, R. *Inorg. Chem.* **2011**, *50*, 10810.

(13) Vargas, V. C.; Rubio, R. J.; Hollis, T. K.; Salcido, M. E. *Org. Lett.* **2003**, *5*, 4847.

(14) CCDC 873530 (**2**), CCDC 873528 (**3**), and CCDC 873529 (**5**) contain the supplementary crystallographic data for this paper. These data can be obtained free of charge from the Cambridge Crystallographic Data Centre via www.ccdc.cam.ac.uk/data_request/cif.

(15) (a) Chianese, A. R.; Li, X.; Janzen, M. C.; Faller, J. W.; Crabtree, R. H. *Organometallics* **2003**, *22*, 1663. (b) Canac, Y.; Lepetit, C.; Abdalilah, M.; Duhayon, C.; Chauvin, R. *J. Am. Chem. Soc.* **2008**, *130*, 8406.

(16) Wu, M. L.; Desmond, M. J.; Drago, R. S. *Inorg. Chem.* **1979**, *18*, 679.

(17) Andrieu, J.; Azouri, M.; Richard, P. *Inorg. Chem. Commun.* **2008**, *11*, 1401.

(18) http://www.ccdc.cam.ac.uk/products/csd/radii/table.php4.

(19) (a) Montang, M.; Schwartsburd, L.; Cohen, R.; Leitus, G.; Ben-David, Y.; Martin, J. M. L.; Milstein, D. *Angew. Chem., Int. Ed.* **2007**, *46*, 1901. (b) Montang, M.; Efremenko, I.; Cohen, R.; Shimon, L. J. W.; Leitus, G.; Diskin-Posner, Y.; Ben-David, Y.; Salem, H.; Martin, J. M. L.; Milstein, D. *Chem.—Eur. J.* **2010**, *16*, 328.

(20) Weinhold, F.; Landis, C. R. In *Valency and Bonding: A Natural Bond Orbital Donor-Acceptor Perspective*; Cambridge University Press: Cambridge, U.K., 2005; pp 480.

(21) Saßmannhausen, J. *Dalton Trans.* **2011**, *40*, 136.

(22) Pregosin, P. S. *Chem. Commun.* **2008**, 4875.

(23) Wood, C. D.; McLain, S. J.; Schrock, R. R. *J. Am. Chem. Soc.* **1979**, *101*, 3210.

(24) Altomare, A.; Cascarano, G.; Giacovazzo, C.; Guagliardi, A.; Burla, M. C.; Polidori, G.; Camalli, M. *J. Appl. Crystallogr.* **1994**, *27*, 435.

(25) Palatinus, L.; Chapuis, G. *J. Appl. Crystallogr.* **2007**, *40*, 786.

(26) Betteridge, P. W.; Carruthers, J. R.; Cooper, R. I.; Prout, K.; Watkin, D. J. *J. Appl. Crystallogr.* **2003**, *36*, 1487.

(27) *International Tables for X-ray Crystallography*; Kynoch Press: Birmingham, England, 1974; Vol. *IV*.

(28) Blessing, R. H. *Acta Crystallogr.* **1995**, *A51*, 33.

(29) Sluis, P. v. d.; Spek, A. L. *Acta Crystallogr.* **1990**, *A46*, 194.

(30) Spek, A. L. *Acta Crystallogr.* **2009**, *D65*, 148.

(31) Frisch, M. J.; Trucks, G. W.; Schlegel, H. B.; Scuseria, G. E.; Robb, M. A.; Cheeseman, J. R.; Scalmani, G.; Barone, V.; Mennucci, B.; Petersson, G. A.; Nakatsuji, H.; Caricato, M.; Li, X.; Hratchian, H. P.; Izmaylov, A. F.; Bloino, J.; Zheng, G.; Sonnenberg, J. L.; Hada, M.; Ehara, M.; Toyota, K.; Fukuda, R.; Hasegawa, J.; Ishida, M.; Nakajima, T.; Honda, Y.; Kitao, O.; Nakai, H.; Vreven, T.; , Jr., Montgomery, J. A.; Peralta, J. E.; Ogliaro, F.; Bearpark, M.; Heyd, J. J.; Brothers, E.; Kudin, K. N.; Staroverov, V. N.; Kobayashi, R.; Normand, J.; Raghavachari, K.; Rendell, A.; Burant, J. C.; Iyengar, S. S.; Tomasi, J.; Cossi, M.; Rega, N.; Millam, N. J.; Klene, M.; Knox, J. E.; Cross, J. B.; Bakken, V.; Adamo, C.; Jaramillo, J.; Gomperts, R.; Stratmann, R. E.; Yazyev, O.; Austin, A. J.; Cammi, R.; Pomelli, C.; Ochterski, J. W.; Martin, R. L.; Morokuma, K.; Zakrzewski, V. G.; Voth, G. A.; Salvador, P.; Dannenberg, J. J.; Dapprich, S.; Daniels, A. D.; Farkas, O.; Foresman, J. B.; Ortiz, J. V.; Cioslowski, J.; and Fox, D. J. *Gaussian 09*, Revision A.1; Gaussian, Inc.: Wallingford, CT, 2009.

(32) Ehlers, A. W.; Böhme, M.; Dapprich, S.; Gobbi, A.; Höllwarth, A.; Jonas, V.; Köhler, K. F.; Stegmann, R.; Veldkamp, A.; Frenking, G. *Chem. Phys. Lett.* **1993**, *208*, 111.
(33) (a) Reed, E. A.; Weinstock, R. B.; Weinhold, F. *J. Chem. Phys.* **1985**, *83*, 735. (b) Reed, E. A.; Weinhold, F. *J. Chem. Phys.* **1985**, *83*, 1736. (c) Reed, E. A.; Curtiss, L. A.; Weinhold, F. *Chem. Rev.* **1988**, *88*, 899.
(34) Glendening, E. D.; Badenhoop, J. K.; Reed, A. E.; Carpenter, J. E.; Bohmann, J. A.; Morales, C. M.; Weinhold, F. *NGO 5.G*; Theoretical Chemistry Institute, University of Wisconsin: Madison, WI, 2001; http://www.chem.wisc.edu/~nbo5
(35) *GABEDIT*; http://sites.google.com/site/allouchear/Home/gabedit.

dx.doi.org/10.1021/ic3006508 | *Inorg. Chem.* 2013, 52, 48−58